

# Electronic Supplementary Information (ESI) for

## Hydrothermally synthesized LiFePO<sub>4</sub> crystals with enhanced electrochemical properties: simultaneous suppression of crystal growth along [010] and antisite defect formation

Xue Qin,<sup>a,b</sup> Jiemin Wang,<sup>a</sup> Jie Xie,<sup>a,b</sup> Fangzhi Li<sup>a</sup>, Lei Wen<sup>a</sup> and Xiaohui Wang<sup>\*a</sup>

<sup>a</sup>Shenyang National Laboratory for Materials Science, Institute of Metal Research, Chinese Academy of Sciences (CAS), Shenyang 110016, China

<sup>b</sup>Graduate School of Chinese Academy of Sciences, Beijing 100039, China

\*Correspondence to

Email: wang@imr.ac.cn

Fax: +86 24 23891620

Tel: +86 24 83970549

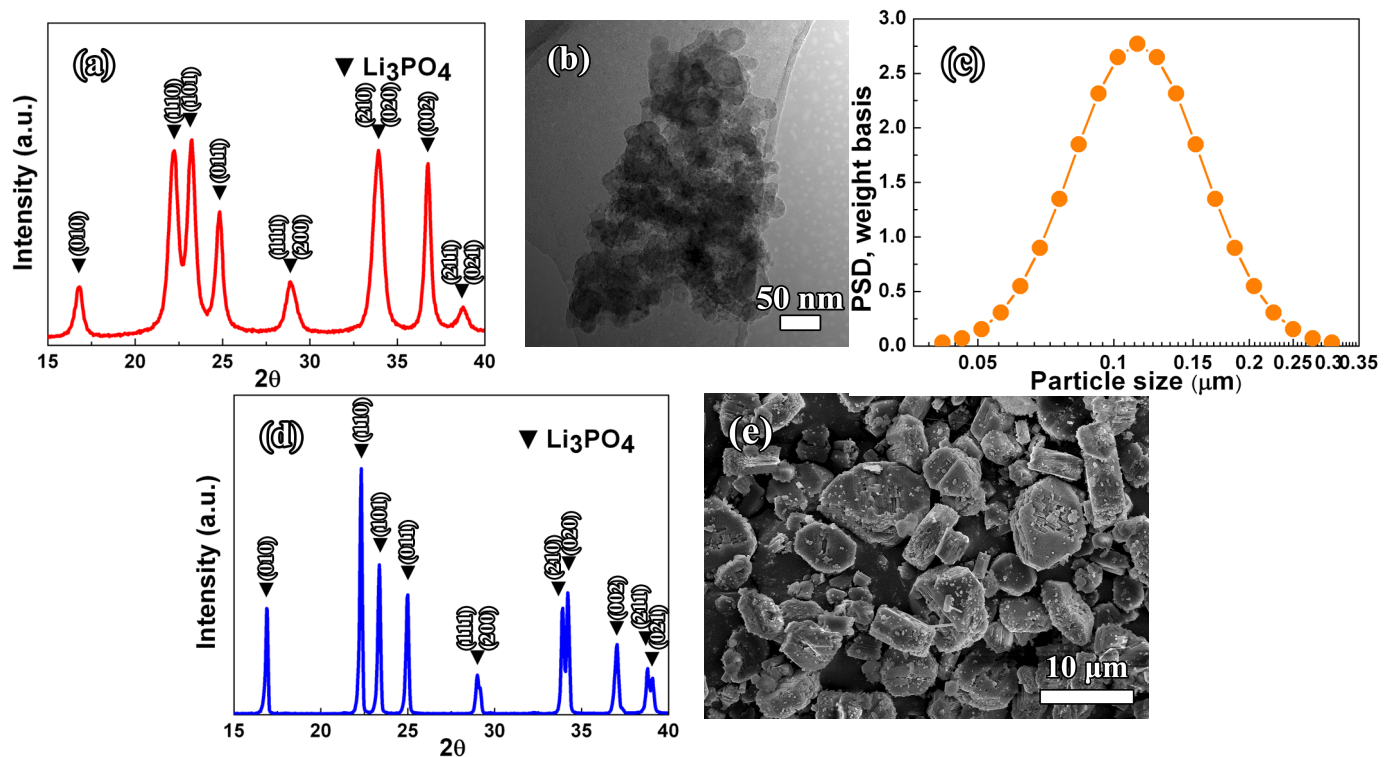


Fig. S1. Characterization of nanosized Li<sub>3</sub>PO<sub>4</sub> obtained by slow addition of H<sub>3</sub>PO<sub>4</sub> into LiOH solution. (a) XRD pattern and (b) TEM image of Li<sub>3</sub>PO<sub>4</sub> before hydrothermal treatment, showing that the formed Li<sub>3</sub>PO<sub>4</sub> consists of shapeless nano-particles. (c) PSD profile, illustrating smaller particle size and good particle size homogeneity. (d) XRD pattern and (e) SEM image of Li<sub>3</sub>PO<sub>4</sub> particles after hydrothermal treatment at 180 °C for 3 h.

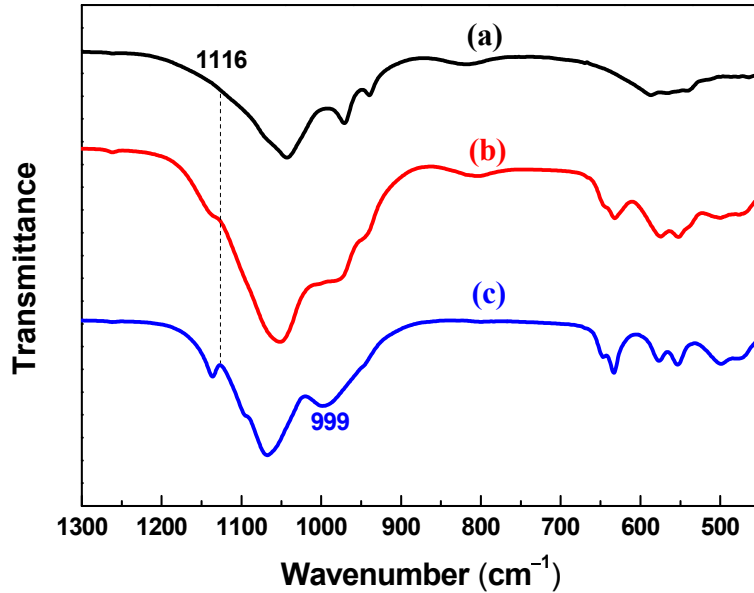


Fig. S2. FTIR spectra of the NP hydrothermally treated up to (a) 135, (b) 140 and (c) 145 °C without holding time, showing the absence of complex composites like tetraphosphate in the NP.

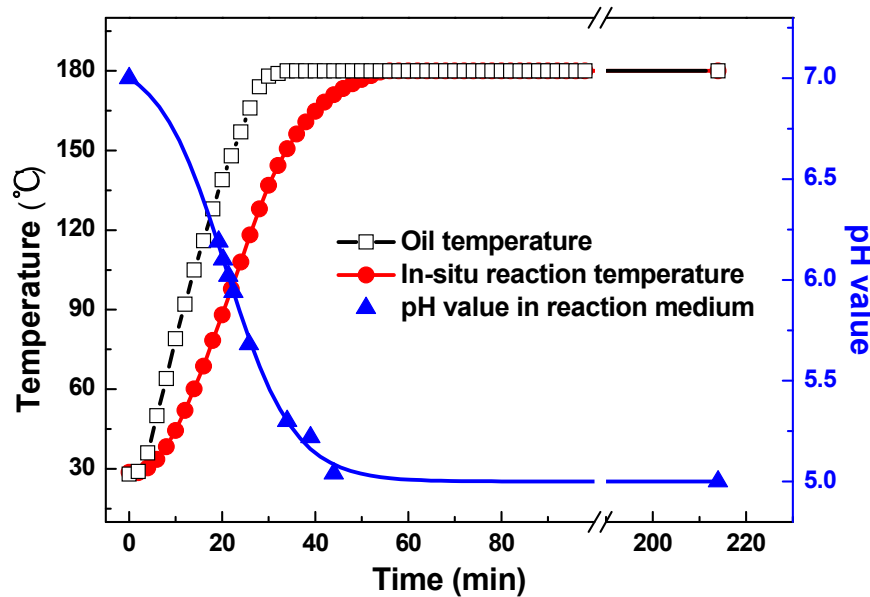


Fig. S3. Evolution of pH values in supernatant. The pH drop is mainly contributed to the decomposition of ascorbic acid and increased amount of  $\text{Li}_2\text{SO}_4$  as the reaction proceeded.

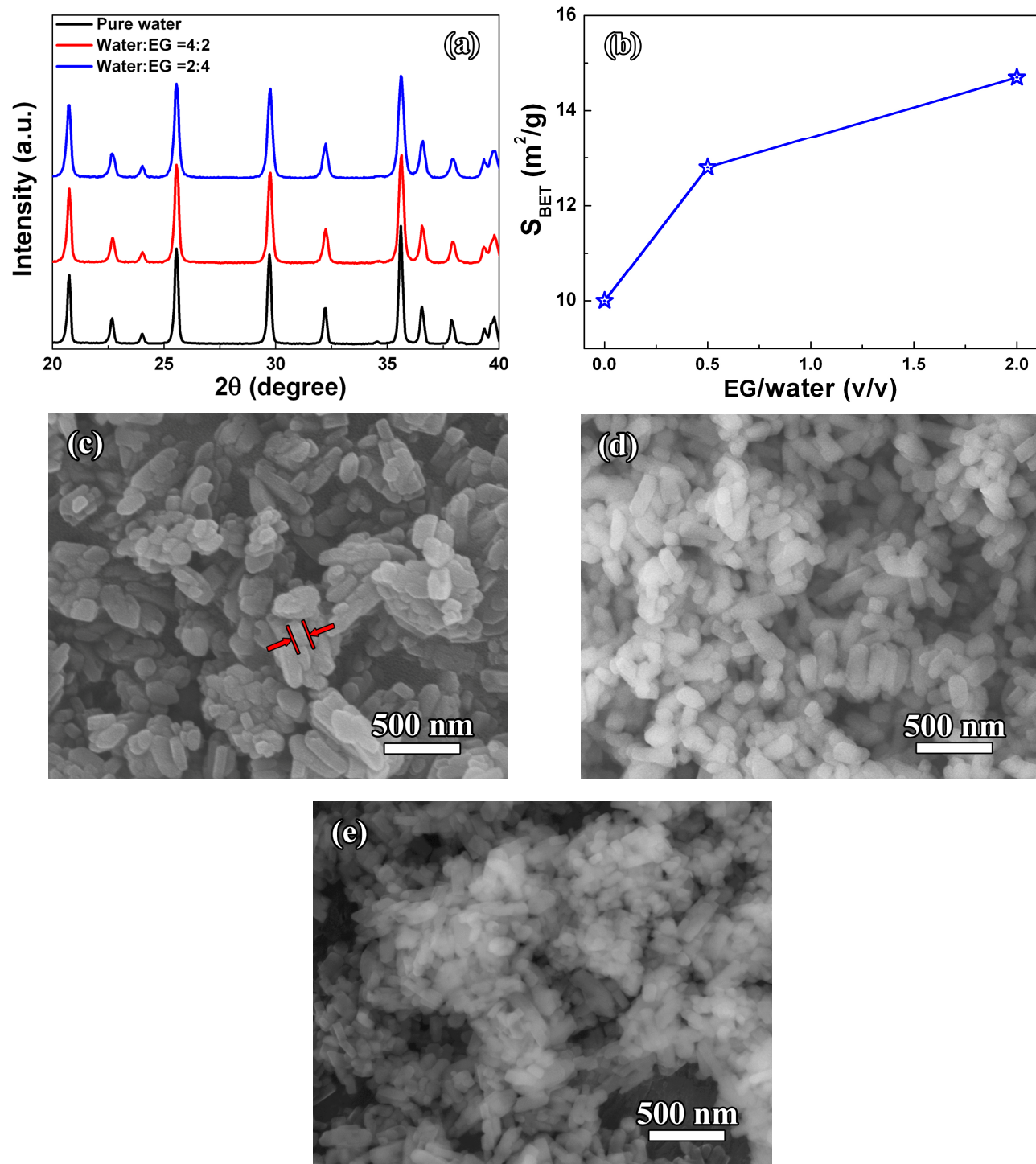


Fig. S4. (a) XRD patterns of LiFePO<sub>4</sub> powders synthesized hydrothermally without EG and with indicated EG contents. (b) dependence of  $S_{BET}$  on EG contents. SEM images of LiFePO<sub>4</sub> powders synthesized (c) in pure water, (d) with water:EG=4:2, and (e) water:EG=2:4 .

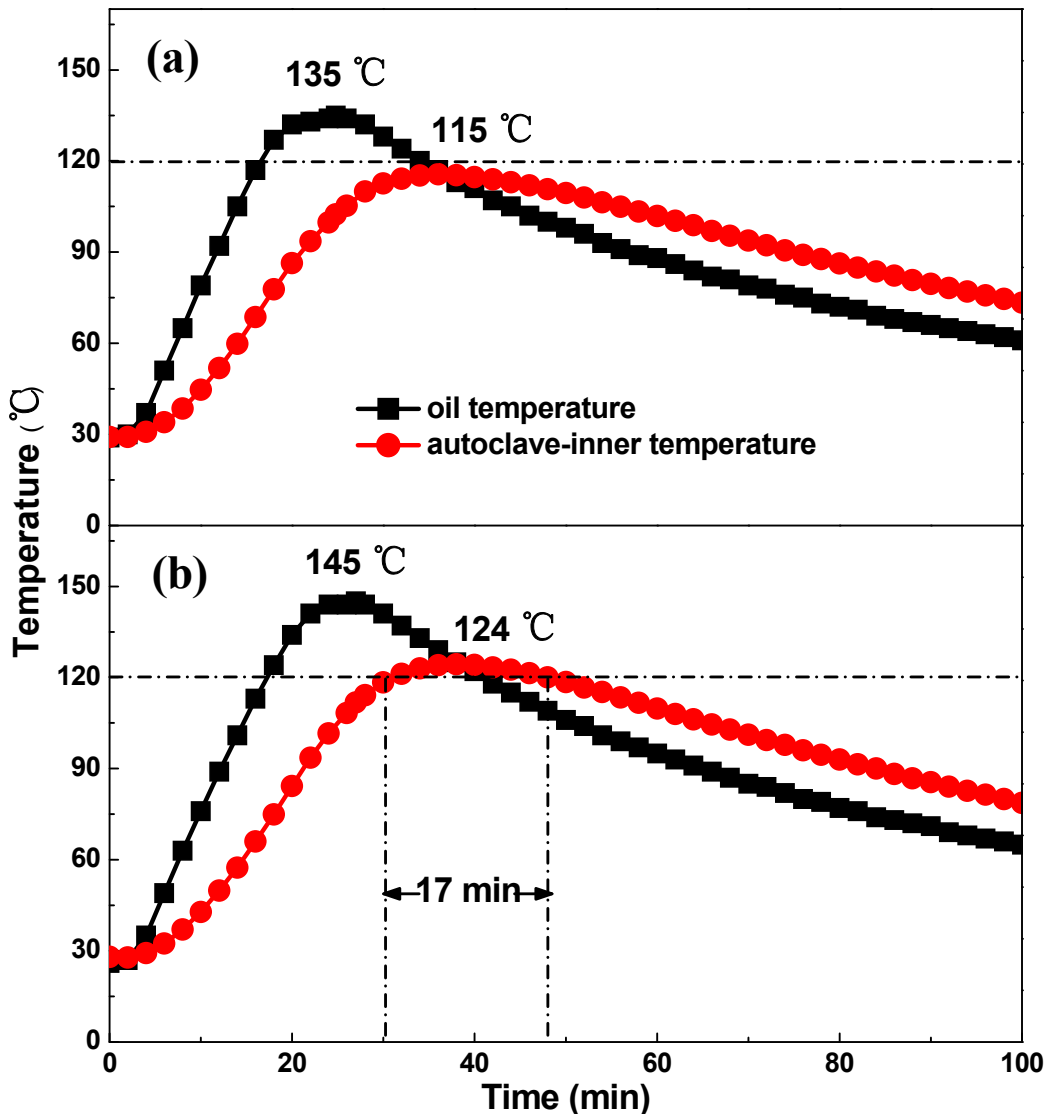


Fig. S5. Comparisons of *in-situ* reaction and oil temperatures against time. Hydrothermally treated up to (a) 135, and (b) 145 °C without holding time. In combination of *in-situ* temperature and XRD phase analysis (Fig. 1a), an ultrafast formation rate for LiFePO<sub>4</sub> hydrothermally synthesized by using NP, is identified.

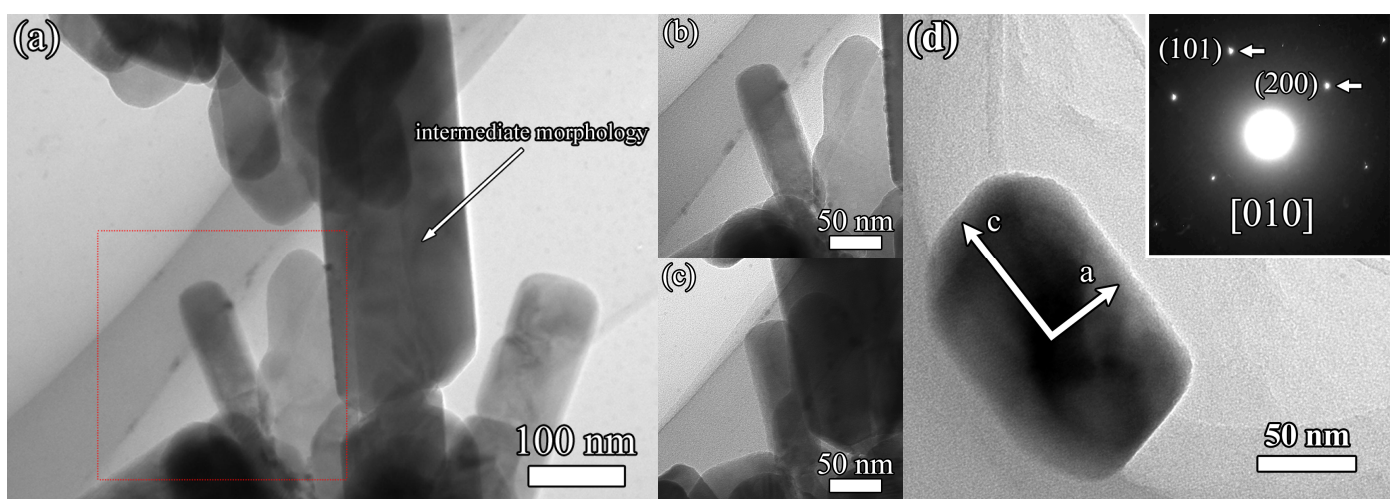


Fig. S6. TEM images. (a) LiFePO<sub>4</sub> crystals synthesized hydrothermally by using NP at 180 °C for 3 h. (b) morphology of the boxed region in (a) before tilting and (c) after tilting 27°, demonstrating typical rod morphology. (d) TEM image of rod-like particle with corresponding crystal growth orientation. Inset shows corresponding SAED pattern with incident beam along the [010] direction.

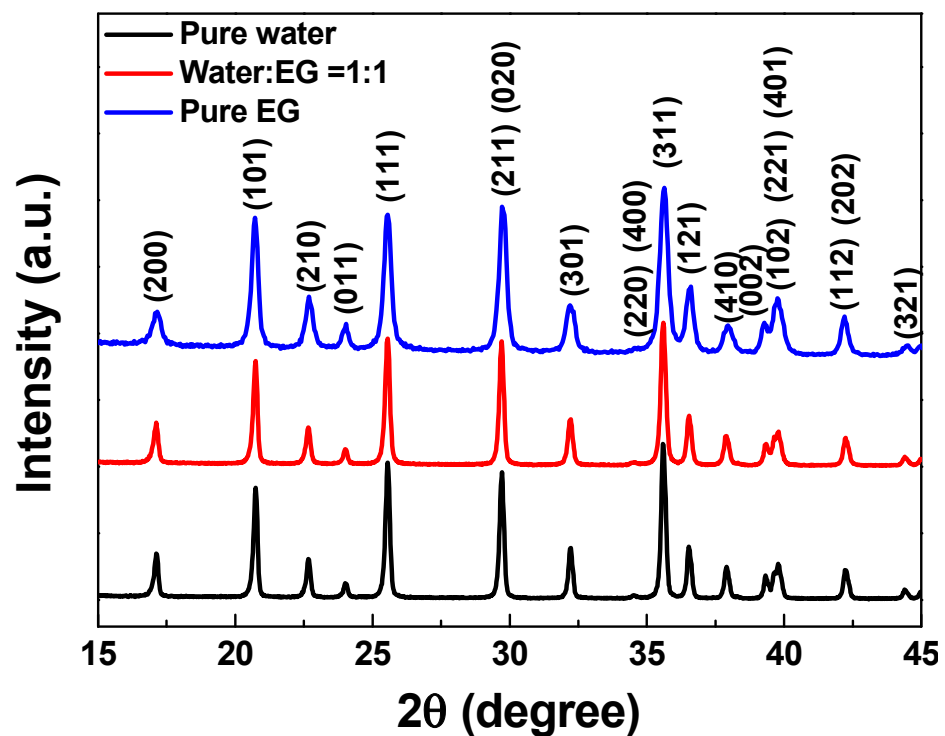


Fig. S7. Powder XRD patterns of LiFePO<sub>4</sub> prepared in different volume ratios of water to EG.

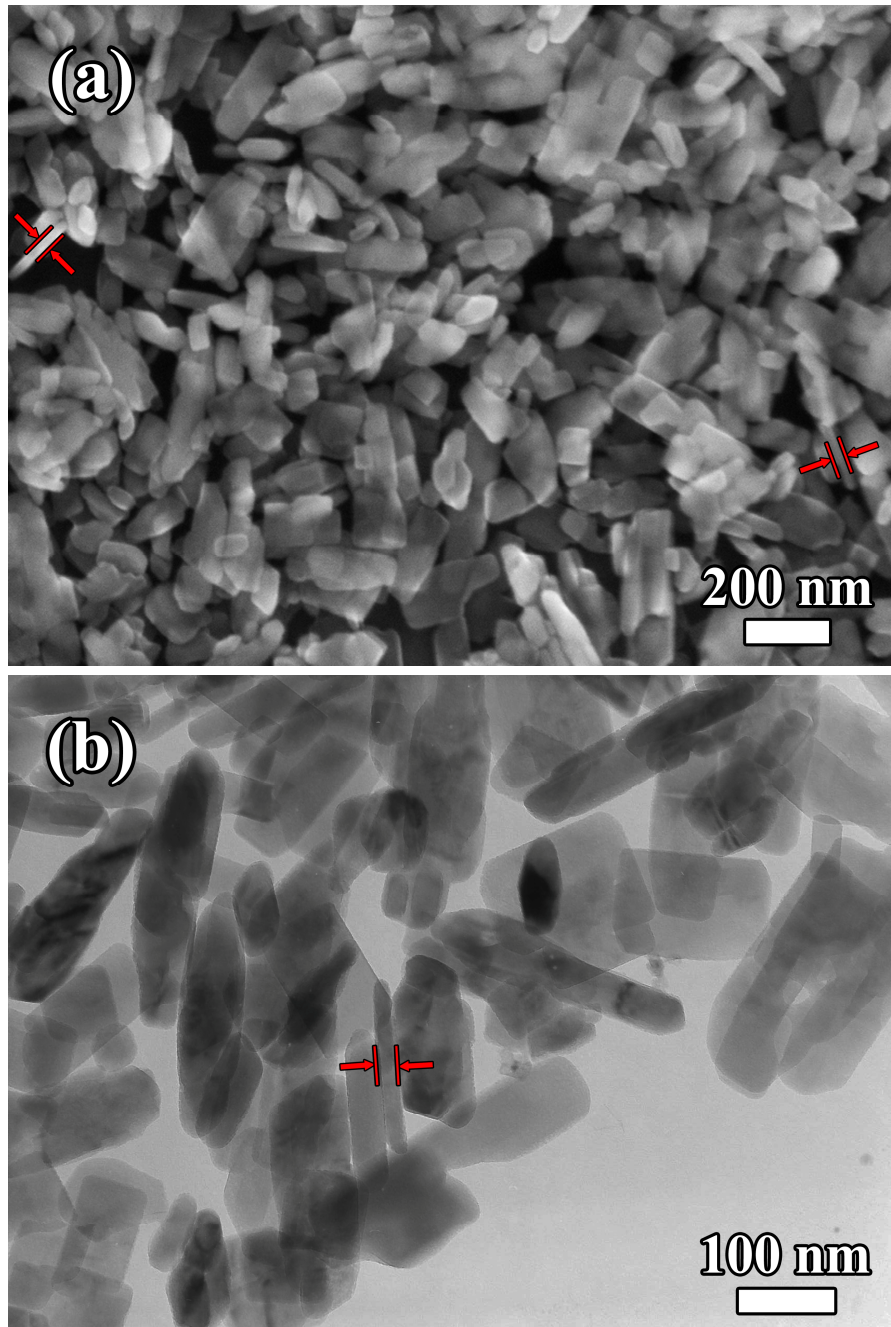


Fig. S8. Typical (a) SEM and (b) TEM images of LiFePO<sub>4</sub> particles synthesized hydrothermally in water/EG (1:1; v/v) system show a few vertical LiFePO<sub>4</sub> particles. In comparison with non-EG-mediated sample with thickness of ~80 nm along [010] crystallographic direction as displayed in Fig. S4c, it shows thinner thickness of ~38 nm and higher S<sub>BET</sub> value of 17.0 m<sup>2</sup> g<sup>-1</sup>.

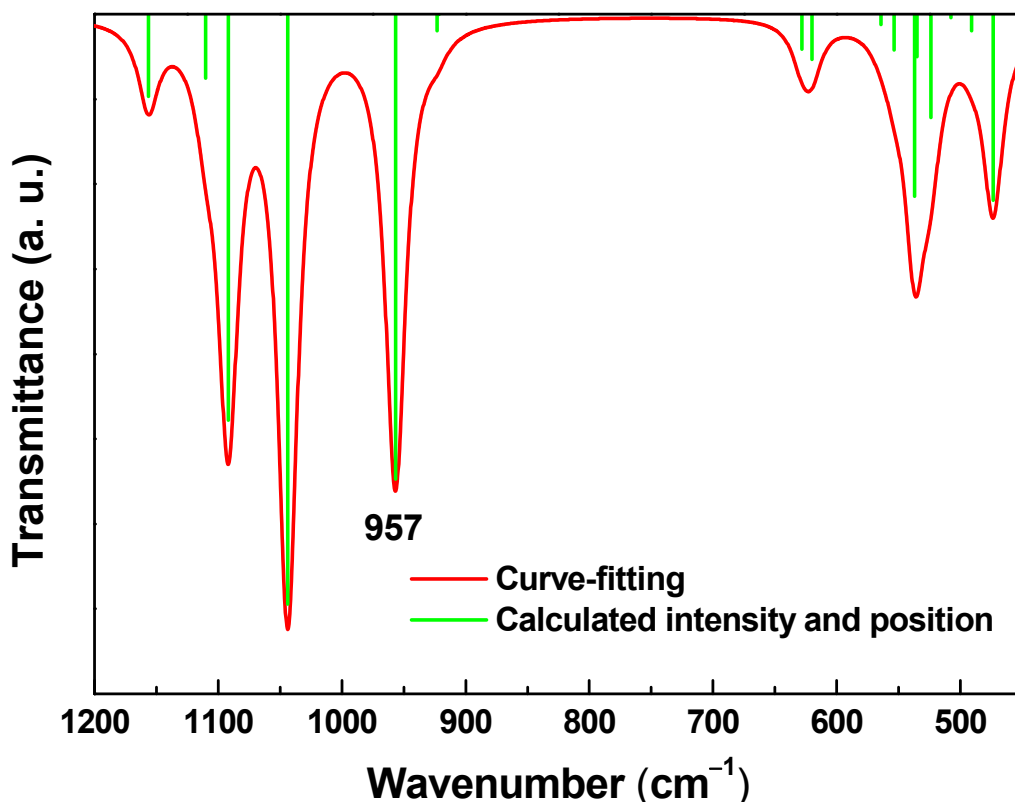


Fig. S9. Calculated FTIR spectrum of defect-free LiFePO<sub>4</sub> using computational simulation technology. The IR vibration modes were obtained from first-principles electronic structure methods based on density functional perturbation theory (DFPT) [1] by using the CASTEP code [2]. The Hellmann-Feynman forces constant matrix was calculated by coupling a standard density functional theory (DFT) with linear response phonon model. The IR intensities were given by the change in electric dipole moment of the system with respect to the atomic motion under excitation of a phonon mode. In the present calculations, the electron-ion interactions were represented by the norm-conserving potentials generated using the kinetic energy optimization scheme developed by Lin *et al.* [3], and Lee [4]. The electronic exchange correlation energy was treated as the generalized gradient approximation (GGA PBE) [5]. The plane wave basis set cut off was 990 eV. The special k-point sampling integration was used over the Brillouin zone by using the Monkhorst-Pack method with 3×4×5 mesh [6].

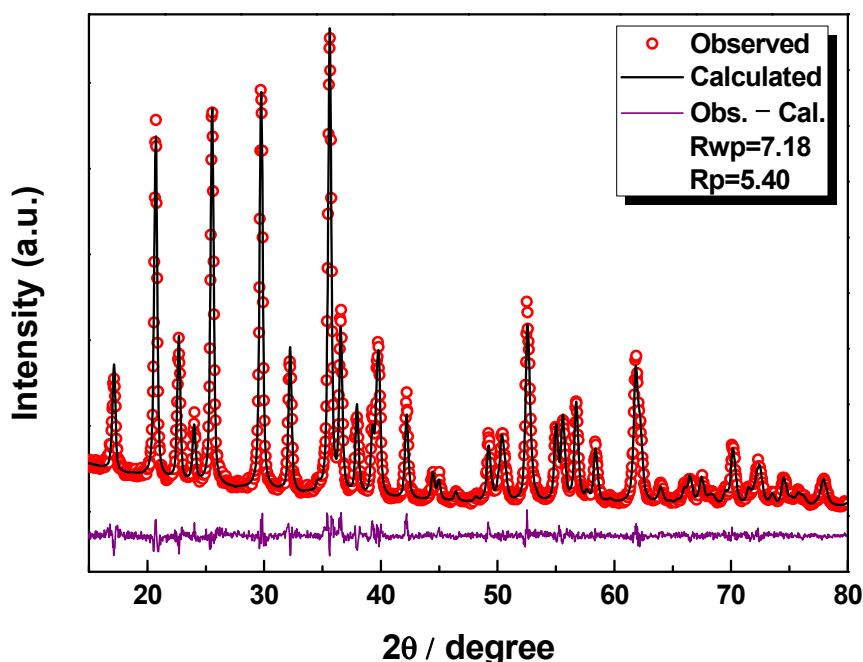


Fig. S10. Rietveld refinement of sample synthesized at 180 °C for 3 h in pure EG reaction system. The result indicates a phase-pure LiFePO<sub>4</sub>. The observed intensity data are shown by red rings, and the black solid line overlying them is the intensity calculated using RIETAN-2000 software. Differences between observed and calculated intensities are plotted by purple solid line. The Rietveld analysis show that lattice constants of olivine structure are  $a=10.3005\pm0.0016$  Å;  $b=5.9895\pm0.0009$  Å;  $c=4.695\pm0.0007$  Å;  $V=289.6\pm0.0738$  Å<sup>3</sup>, respectively. The model considers [010] preferred-orientation as a result of the very thin crystal thickness along [010] crystallographic direction.

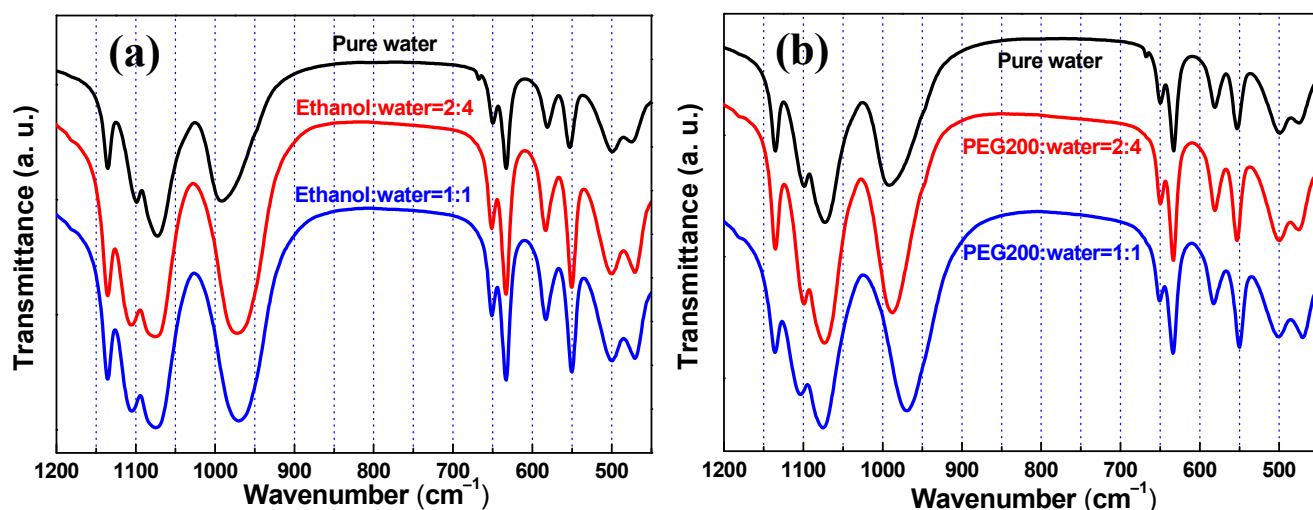
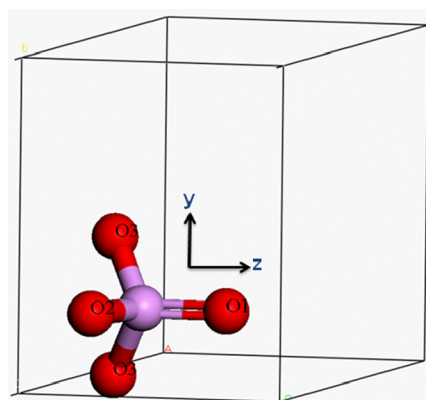


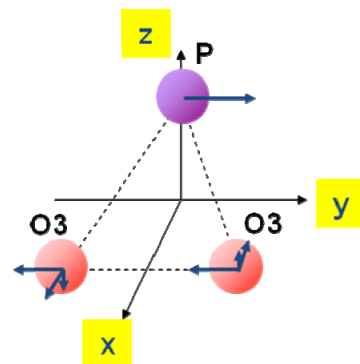
Fig. S11. FTIR spectra of LiFePO<sub>4</sub> prepared by introducing various amounts of (a) ethanol (b) polyethylene-glycol(200) (PEG200).

Table S1. Calculated atomic vibrations and force constants in phosphate group along different direction while a few Li sites were occupied by divalent Fe ions.

Atom	P	O1	O2	O3	O3
$\Delta x$	0	0	0	0.126	-0.126
$\Delta y$	0.315	-0.006	-0.003	-0.223	-0.223
$\Delta z$	0	0	0	-0.095	0.095



	x	y	z
Perfect crystal	51.2	45.5	64.0
FeLi antisite defects	48.0	53.0	64.5



Compared with almost unvibrated O1 and O2, the calculated results suggest that the obvious vibrations of atom P and O3 along different direction occur when the  $\text{Fe}_{\text{Li}}^+$  antisite defects form. Therefore, we further calculate the force constants of P and O3 along different directions. The force constants were calculated by the finite displacement method. When given a small nonequivalent displacement on an atom along the specific direction, the atomic Hellmann-Feynman forces was obtained by VASP [7, 8], which is a density functional theory (DFT) total energy calculation code. The employed  $1 \times 2 \times 2$  supercell contains 112 atoms. A  $2 \times 2 \times 3$   $k$ -point mesh and 550 eV energy cutoff were used when calculating the Hellmann-Feynman forces in the supercell. The electron-ion interactions were represented by the projector augmented wave (PAW) method [9]. The electronic exchange-correlation energy was treated as the generalized gradient approximation (GGA PBE) [5]. Considering y direction is dominating vibration direction, we believe that the force constants of phosphate group increase when the  $\text{Fe}_{\text{Li}}^+$  antisite defects form.

## References:

- [1] S. Baroni, S. de Gironcoli, A. Dal Corso and P. Giannozzi, *Rev. Mod. Phys.*, 2001, **73**, 515.
- [2] M. D. Segall, P. L. D. Lindan, M. J. Probert, C. J. Pickard, P. J. Hasnip, S. J. Clark and M. C. Payne, *J Phy-Condens. Mat.*, 2002, **14**, 2717.
- [3] J. S. Lin, A. Qteish, M. C. Payne and V. Heine, *Phys. Rev. B*, 1993, **47**, 4174.
- [4] M. H. Lee, Ph.D. Thesis, Cambridge University, 1996.
- [5] J. P. Perdew, K. Burke and M. Ernzerhof, *Phys. Rev. Lett.*, 1996, **77**, 3865.
- [6] H. J. Monkhorst and J. D. Pack, *Phys. Rev. B*, 1977, **16**, 1748.
- [7] G. Kresse and J. Hafner, *Phys. Rev. B*, 1993, **47**, 558.
- [8] G. Kresse and J. Furthmüller, *Phys. Rev. B*, 1996, **54**, 11169.
- [9] G. Kresse and J. Joubert, *Phys. Rev. B*, 1999, **59**, 1758.